Structural and Kinetic Considerations for the Application of the Traceless Staudinger Ligation to Future ^{18}F Radiolabeling Using XRD and ^{19}F NMR

MARTIN KÖCKERLING,[1] CONSTANTIN MAMAT[2]

[1]*Institut für Chemie, Anorganische Festkörperchemie, Universität Rostock, D-18059, Rostock, Germany*

[2]*Institut für Radiopharmazeutische Krebsforschung, Helmholtz-Zentrum Dresden-Rossendorf, D-01328, Dresden, Germany*

Received 4 March 2017; revised 19 October 2017; accepted 19 October 2017

DOI 10.1002/kin.21137
Published online in Wiley Online Library (wileyonlinelibrary.com).

ABSTRACT: A 4-fluorobenzoate-functionalized phosphane was synthesized and reacted with different azides using the traceless Staudinger ligation as a representative sample reaction for future radiolabeling purposes with short-lived radionuclides like fluorine-18. For this purpose, the reaction rate was evaluated at different temperatures. The effect of starting material concentrations and the influence of the steric effect coming from the applied azides were investigated. ^{19}F NMR was used to determine the reaction half-live ($\tau_{1/2}$) and the reaction rate constant (k_{obs}) of this ligation under mild reaction conditions in a water–acetonitrile mixture. Furthermore, the phosphane key compound **1** (orthorhombic, space group $Pna2_1$, $a = 18.6363(9)$, $b = 8.3589(4)$, $c = 18.5480(9)$ Å, $V = 2889.4(2)$ Å^3, $Z = 8$, $D_{obs} = 1.277$ g/cm^3), which acts as starting material for all subsequent syntheses, and the fluorine-containing phosphane **3** (monoclinic, space group $P2_1/c$, $a = 8.321(2)$, $b = 16.160(4)$, $c = 14.940(4)$ Å, $\beta = 99.51(1)°$, $V = 1981.4(8)$ Å^3, $Z = 4$, $D_{obs} = 1.342$ g/cm^3) were analyzed by single-crystal XRD. © 2017 Wiley Periodicals, Inc. Int J Chem Kinet 1–10, 2017

INTRODUCTION

Both variants of Staudinger ligation [1] belong to the most important bioorthogonal conjugation reactions for site-selective labeling purposes [2,3] and

Correspondence to: Constantin Mamat; e-mail: c.mamat@hzdr.de.

Supporting Information is available in the online issue at www.wileyonlinelibrary.com.

proceed without any catalyst in contrast to other reactions (e.g., the Huisgen click reaction) [4]. The absence of a metal catalyst (e.g., Cu) is important especially for in vitro and in vivo applications, because Cu is known to be cytotoxic [5]. Therefore, the traceless variant of the Staudinger ligation [6–8] independently developed by Raines et al. [9] and Bertozzi et al. [10] is employed for several applications in chemistry, biochemistry, and (radio)pharmacy. The connection of proteins [11,12], peptides, and peptide fragments [9,13], the glycosylation [14] of amino acids and peptides [15,16], the preparation of large-sized lactams [17,18], the functionalization of polymers [19], and the introduction of radiolabels [20–23] as well as fluorescence dyes [24–26] makes this reaction widely applicable. Both the chemical modification of the biological active molecule and the preparation of the labeling building block are also quite facile. In general, one of the reactants is modified with an azide function [27,28] and the other is functionalized with a phosphane moiety [29,30].

Knowledge about the reaction rate of the traceless Staudinger ligation in particular for radiolabeling purposes is beneficial, since the applied radionuclides often suffer from short half-live (e.g., ^{11}C: 20 min, ^{18}F: 110 min, ^{99m}Tc: 6 h) [31]. Thus, a short reaction time under mild reaction conditions (e.g., low reaction temperature, aqueous reaction medium) is crucial especially for the introduction of radiolabels into sensitive bio(macro)molecules like proteins or antibodies [32,33].

In the past, NMR was used to study the mechanism and the reaction rate of the Staudinger ligation [34,35], but costly ^{13}C-labeled starting materials were used to quantitatively determine the spectra in a reasonable time span. To avoid performing circumstantial syntheses for the preparation of the ^{13}C-enriched starting materials and/or long-lasting measurements, we focused on the application of ^{19}F NMR, since ^{19}F-containing derivatives were mandatory to prepare as reference compounds for the identification of the corresponding ^{18}F radiotracers and, therefore, they were already available [36]. Advantageously, ^{19}F NMR measurements are simply to perform nowadays, and the progress of the reaction can easy be monitored, because the ^{19}F nucleus is present in the starting material and also in the ligation product. In our case, the fluorine-containing phosphane **3** acts as starting material and gives amides **7–9** as ligation products.

Fluorine-19 has favorable properties for NMR measurements like a nuclear spin of 1/2, a high gyromagnetic ratio (0.94 × of ^{1}H), and it is 100% naturally enriched as ^{19}F (monoisotopic) [37], which makes this isotope highly responsive for fast and quantitative NMR measurements in the same manner as ^{1}H or ^{31}P. No supplemental introduction or enrichment of NMR sensitive nuclides into one or both of the reactants is mandatory in contrast to ^{12}C/^{13}C measurements. In the past, ^{19}F NMR has been used as an excellent tool for kinetic studies on chemical reactions [38,39].

Our first objective was the structure elucidation of fluorine-containing phosphane, which acts as starting material for the traceless Staudinger ligation to introduce the 4-fluorobenzoate moiety. Our second objective was to develop a convenient method to determine the reaction rate of this ligation reaction via ^{19}F NMR. The obtained results give an impression to make a prediction for future applications of this ligation method for mild radiolabeling with the β^+-emitter fluorine-18.

EXPERIMENTAL

General

Phosphanes **1**, **3**, **5** [29] and azide **4** [40] were synthesized as reported in the literature. NMR spectra of all compounds were recorded on an Agilent DD2-600 MHz NMR spectrometer (ProbeOne) at 25 and 45°C (Agilent Technologies, Waldronn, Germany). Chemical shifts of the ^{1}H, ^{13}C, and ^{31}P spectra were reported in parts per million (ppm) using TMS as internal standard for ^{1}H and ^{13}C, $CFCl_3$ for ^{19}F, and H_3PO_4 for ^{31}P spectra. The assignment was further verified by two-dimensional measurements (H,H-COSY, HSQC). Deuterated solvents (C_6D_6, CD_3CN, D_2O) were purchased from Deutero (Kastellaun, Germany). For the first kinetic NMR experiment, stock solutions of phosphane **3** were prepared with a concentration of 71 mM and azide **4** with final concentrations of 71 mM and 710 mM, respectively, using a mixture of CD_3CN and D_2O (v:v = 10:1). 300 μL of each solution was combined into an NMR tube to reach a final solvent amount of 600 μL. The reaction of **3** with fructose derivatives **5** and **6** was done according to the same procedure but with lower concentrations due to solubility reasons (**3**: 17.7 mM, **5**: 187.4 mM, **6**: 176.4 mM). At the beginning of the reaction, ^{19}F and ^{31}P NMR spectra were recorded all 3–15 min, later all 30–60 min. In all experiments, 16 scans were recorded for the recording of the ^{19}F and ^{31}P spectra. Measurements were accomplished using the standard pulse sequence from OpenVnmrJ software. Determined signals were integrated, and the values were plotted versus time. Logarithmic plotting was used to determine the reaction half-life $\tau_{1/2}$ and the rate constant k_{obs} of the reaction. The concentration dependence of the OH group in **3** was determined using a stock solution

(72.3 mM) of **3** in C_6D_6, which was diluted using 300 μL stock solution and 300 μL C_6D_6 (except the last: 300 μL stock solution + 900 μL C_6D_6). All NMR experiments were performed in triplicate. Diffraction data were collected with a Bruker-Nonius-Apex-II-diffractometer using graphite-monochromated Mo Kα radiation (λ = 0.71073 Å). All diffraction measurements were done at –150°C. The unit cell dimensions were recorded and refined using the angular settings of 7238 (**1**), and 9338 (**3**) reflections, and the structures were solved by direct methods and refined against F^2 on all data by full-matrix least-squares using the program suits from Sheldrick [41–43]. All nonhydrogen atoms were refined anisotropically; all hydrogen atoms were placed on geometrically calculated positions and refined using a riding model. CCDC 1482485 (**1**) and CCDC 1482528 (**3**) contain the supplementary crystallographic data for this paper. These data can be obtained free of charge from The Cambridge Crystallographic Data Centre via www.ccdc.cam.ac.uk/data_request/cif.

Chemistry

1-(6-Azidohexanamido)-1-deoxy-2,3:4,5-di-O-isopropylidene-β-D-fructopyranose (6). 6-Azidohexanoic acid (197 mg, 1.25 mmol), 2,3:4,5-di-*O*-isopropylidene-β-D-fructopyranose (398 mg, 1.52 mmol), EDC·HCl (347 mg, 1.81 mmol), and *N*,*N*-dimethylaminopyridine in catalytic amounts were dissolved in anhydrous THF (8 mL), and the mixture was heated under stirring at 50°C for 6 h. After TLC control, the solids were filtered, the solvent was removed, and the crude product was purified via column chromatography (petroleum ether: ethyl acetate = 10:1) to yield **6** (249 mg, 50%) as colorless syrup. R_f = 0.6 (petroleum ether: ethyl acetate = 3:2); ^{1}H NMR ($CDCl_3$): δ 1.33 (s, 3H, CH_3), 1.36–1.45 (m, 5H, CH_2+CH_3), 1.47 (s, 3H, CH_3), 1.53 (s, 3H, CH_3), 1.56–1.72 (m, 4H, CH_2), 2.37 (t, ^3J = 7.5 Hz, 2H, CH_2C=O), 3.26 (t, ^3J = 6.8 Hz, 2H, CH_2N_3), 3.75 (d, ^3J = 13.0 Hz, 1H, H-6a), 3.90 (dd, ^3J = 13.0 Hz, ^4J = 1.5 Hz, 1H, H-6b), 4.03 (d, ^3J = 11.8 Hz, 1H, H-1a), 4.23 (dd, ^3J = 7.9 Hz, ^4J = 1.5 Hz, 1H, H-5), 4.29 (d, ^3J = 2.6 Hz, 1H, H-3), 4.40 (d, ^3J = 11.8 Hz, 1H, H-1b), 4.59 (dd, ^3J = 2.6 Hz, ^3J = 7.9 Hz, 1H, H-4); ^{13}C NMR: δ 24.2 (CH_3), 24.4 (CH_2), 25.4 (CH_3), 26.0 (CH_3), 26.4 (CH_2), 26.6 (CH_3), 28.7 (CH_2), 34.0 (CH_2C=O), 51.3 (CH_2N_3), 61.4 (C-6), 65.4 (C-1), 70.2 (C-4), 70.7 (C-3), 70.9 (C-5), 101.7 (C-2), 108.8 (C-q), 109.3 (C-q), 172.8 (C=O); MS (ESI+) *m/z*: 399 [M^++H]; Anal. calcd for $C_{18}H_{30}N_4O_6$ (398.22): C, 54.26; H, 7.59; N, 14.06. Found: C, 53.99; H, 7.55; N, 14.19.

1-(4-Fluorobenzamido)-1-deoxy-2,3:4,5-di-O-isopropylidene-β-D-fructopyranose (8). Compounds **3** (50 mg, 0.12 mmol) and **5** (36 mg, 0.12 mmol) were dissolved in a mixture of acetonitrile and water (1.1 mL, 10:1), and the resulting solution was heated at 40°C for 6 h. Afterwards, the solvent was removed and the crude product was purified via column chromatography (petroleum ether: ethyl acetate = 10:1) to yield **8** (40 mg, 84%) as colorless syrup. R_f = 0.6 (petroleum ether: ethyl acetate = 3:2); ^{1}H NMR ($CDCl_3$): δ 1.30 (s, 3H, CH_3), 1.32 (s, 3H, CH_3), 1.40 (s, 3H, CH_3), 1.53 (s, 3H, CH_3), 3.68–3.77 (m, 2H, H-1a, H-6a), 3.82–3.92 (m, 2H, H-1b, H-6b), 4.21 (dd, ^3J = 7.8 Hz, ^4J = 1.7 Hz, 1H, H-5), 4.36 (d, ^3J = 2.5 Hz, 1H, H-3), 4.58 (dd, ^3J = 2.5 Hz, ^3J = 7.8 Hz, 1H, H-4); 6.69 (br s, 1H, NH), 7.08 (t, $^3J_{o,m}$ = $^3J_{H,F}$ = 8.6 Hz, 2H, H_m), 7.80 (dd, $^4J_{H,F}$ = 5.4 Hz, $^3J_{o,m}$ = 8.6 Hz, 2H, H_o); ^{13}C (400 MHz, $CDCl_3$): δ 24.1, 25.1, 26.0, 26.2 (4 × CH_3), 47.6 (C-1), 61.6 (C-6), 65.4 (C-1), 70.4 (C-4), 70.6 (C-5), 72.1 (C-3), 102.8 (C-2), 108.7 (C-q), 109.2 (C-q), 115.5 (d, $^2J_{C,F}$ = 21.9 Hz, C_m), 129.6 (d, $^3J_{C,F}$ = 8.7 Hz, C_o), 164.7 (d, $^1J_{C,F}$ = 250.3 Hz, C_p), 166.9 (C_i + C=O); MS (ESI+) *m/z*: 382 [M^++H]; Anal. calcd for $C_{19}H_{24}FNO_6$ (381.40): C, 59.83; H, 6.34; N, 3.67. Found: C, 60.01; H, 6.23; N, 3.71.

1-(6-(4-Fluorobenzamido)hexanamido)-1-deoxy-2,3:4,5-di-O-isopropylidene-β-D-fructopyranose (9). Compounds **3** (47 mg, 0.12 mmol) and **6** (47 mg, 0.12 mmol) were dissolved in a mixture of acetonitrile and water (1.1 mL, 10:1), and the resulting solution was heated at 40°C for 6 h. Afterwards, the solvent was removed and the crude product was purified via column chromatography (petroleum ether: ethyl acetate = 2:1) to yield **9** (50 mg, 86%) as colorless syrup. R_f = 0.6 (petroleum ether: ethyl acetate = 3:2); ^{1}H NMR (400 MHz, $CDCl_3$): δ 1.33 (s, 3H, CH_3), 1.36–1.45 (m, 5H, CH_2+CH_3), 1.47 (s, 3H, CH_3), 1.53 (s, 3H, CH_3), 1.60–1.74 (m, 4H, CH_2), 2.38 (t, ^3J = 7.1 Hz, 2H, CH_2C=O), 3.45 (dt, ^3J = 6.7 Hz, 2H, CH_2NH), 3.76 (d, ^3J = 13.2 Hz, 1H, H-6a), 3.90 (dd, ^3J = 13.2 Hz, ^4J = 1.5 Hz, 1H, H-6b), 4.03 (d, ^3J = 11.6 Hz, 1H, H-1a), 4.23 (dd, ^3J = 7.7 Hz, ^4J = 1.5 Hz, 1H, H-5), 4.29 (d, ^3J = 2.4 Hz, 1H, H-3), 4.41 (d, ^3J = 11.6 Hz, 1H, H-1b), 4.60 (dd, ^3J = 2.4 Hz, ^3J = 7.7 Hz, 1H, H-4), 6.24 (br s, 1H, NH), 7.09 (t, $^3J_{o,m}$ = $^3J_{H,F}$ = 8.7 Hz, 2H, H_m), 7.78 (dd, $^4J_{H,F}$ = 5.3 Hz, $^3J_{o,m}$ = 8.7 Hz, 2H, H_o); ^{13}C NMR (400 MHz, $CDCl_3$): δ 24.2 (CH_3), 24.3 (CH_2), 25.4 (CH_3), 26.0 (CH_3), 26.5 (CH_2), 26.6 (CH_3), 29.3 (CH_2), 34.0 (CH_2C=O), 39.9 (CH_2NH), 61.4 (C-6), 65.4 (C-1), 70.2 (C-4), 70.7 (C-3), 70.9 (C-5), 101.7 (C-2), 108.9 (C-q), 109.3 (C-q), 115.7 (d, $^2J_{C,F}$ = 21.8 Hz,

C_m), 129.3 (d, $^3J_{C,F}$ = 9.3 Hz, C_o), 164.8 (d, $^1J_{C,F}$ = 251.3 Hz, C_p), 166.6 (C_i), 173.0 (C=O); ^{19}F NMR (376 MHz, $CDCl_3$): δ –108.6; MS (ESI+) *m/z*: 495 [M^++H]; Anal. calcd for $C_{25}H_{35}FN_2O_7$ (494.56): C, 60.72; H, 7.13; N, 5.66. Found: C, 60.61; H, 7.09; N, 5.45.

2-(Diphenylphosphoryl)phenyl 4-fluorobenzoate (11). Compound **3** (100 mg, 0.25 mmol) and NaN_3 (32 mg, 0.5 mmol) were dissolved in a mixture of acetonitrile and water (300 µL, 10:1), and the resulting solution was heated at 40°C for 6 h. Afterwards, the solvent was removed and the crude product was purified via column chromatography (petroleum ether: ethyl acetate = 10:1) to yield **11** (88 mg, 85%) as colorless syrup. R_f = 0.3 (petroleum ether:ethyl acetate = 3:1); ^{1}H NMR (400 MHz, C_6D_6): 6.56 (t, $^3J_{o,m}$ = $^3J_{H,F}$ = 8.8 Hz, 2H, $H_{m(F)}$), 6.76 (t, ^3J = 7.5 Hz, 1H, H-4), 6.87–6.99 (m, 6H, H-Ar), 7.08 (t, ^3J = 7.7 Hz, 1H, H-5), 7.22 (dd, J = 4.3 Hz, ^3J = 8.4 Hz, 1H, H-6), 7.37 (dd, ^3J = 7.5 Hz, J = 12.9 Hz, 1H, H-3), 7.69–7.77 (m, 4H, Ar), 7.87 (dd, $^4J_{H,F}$ = 5.6 Hz, $^3J_{o,m}$ = 8.8 Hz, 2H, $H_{o(F)}$); ^{13}C NMR (C_6D_6): δ 115.4 (d, $^3J_{C,F}$ = 22.4 Hz, $C_{o(F)}$), 124.5 (d, $^3J_{C,P}$ = 5.7 Hz, C-6), 125.8 (d, $^3J_{C,P}$ = 11.2 Hz, C-4), 127.0 (d, $^1J_{C,P}$ = 100.1 Hz, C-2), 128.5 (d, $^3J_{C,P}$ = 12.2 Hz, $C_{m(P)}$), 131.6 (d, $^4J_{C,P}$ = 2.5 Hz, $C_{p(P)}$), 132.1 (d, $^2J_{C,P}$ = 9.7 Hz, $C_{o(P)}$), 133.3 (d, $^4J_{C,P}$ = 2.2 Hz, C-5), 133.5 (d, $^2J_{C,F}$ = 9.7 Hz, $C_{m(F)}$), 134.2 (d, $^1J_{C,P}$ = 104.5 Hz, $C_{i(P)}$), 134.5 (d, $^2J_{C,P}$ = 8.6 Hz, C-3), 153.6 ($C_{i(F)}$), 162.9 (C=O), 166.2 (d, $^1J_{C,F}$ = 254.3, $C_{p(F)}$); ^{19}F NMR (376 MHz, C_6D_6): δ –105.1; ^{31}P NMR (C_6D_6): 23.3; MS (ESI+) *m/z*: 417 [M^++H]; Anal. calcd for $C_{25}H_{18}FO_3P$ (416.39): C, 72.11; H, 4.36. Found: C, 72.17; H, 4.29.

RESULTS AND DISCUSSION

Synthesis and X-Ray Determination

Independent on the variant of the Staudinger ligation (traceless or nontraceless), functionalized phosphanes act as starting material in general [6–8]. Furthermore, the traceless ligation can be divided in two approaches. In the direct approach, the imaging probe (radionuclide, fluorescent dye, etc.) is connected to the phosphane moiety whereas the imaging probe is connected to the azide and the phosphane is connected to the molecule to be labeled in the indirect approach.

Especially for the traceless variant, phosphanes like **3** with an electrophilic center (e.g., ester, thioester, amide) in close proximity to the phosphorus are required. For this purpose, phosphane **3** [29] was prepared by the reaction of phosphane **1** with 4-fluorobenzoyl chloride (**2**) under basic conditions [44,45]. The reaction is shown in Scheme 1.

Phosphane **1** acts as a basic starting compound to prepare further functionalized derivatives for ligation purposes. Single crystals of **1** and **3** were obtained during the purification process and were characterized by single crystal X-ray analysis [41–43]. The molecular structures of both phosphanes are illustrated in Figs. 1 and 2.

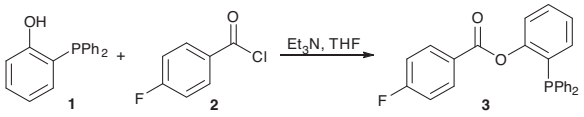

Scheme 1 Synthesis of the fluorine containing phosphane building block **3** by the reaction of phosphane **1** and 4-fluorobenzoyl chloride (**2**).

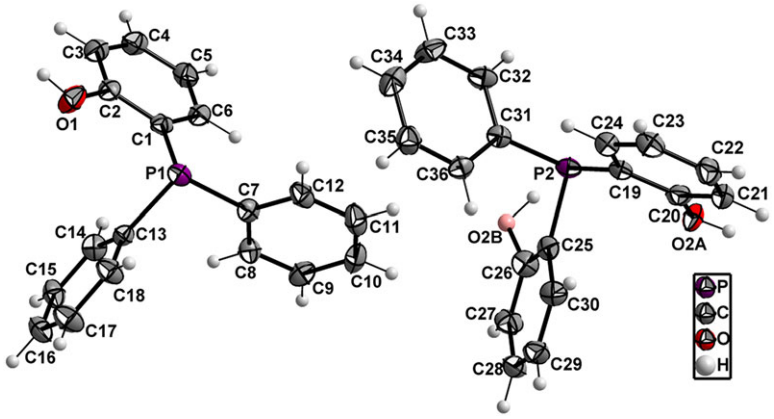

Figure 1 Structure of the two symmetry independent molecules of the phosphane **1** (ORTEP plot, 50% probability level). [Color figure can be viewed at wileyonlinelibrary.com]

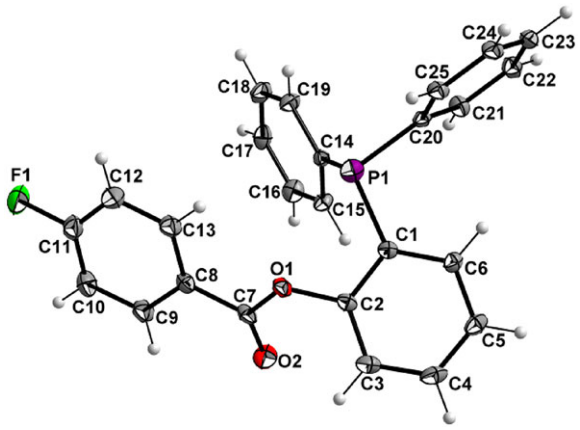

Figure 2 Molecular structure of the fluorine-containing phosphane **3** (ORTEP plot, 50% probability level). [Color figure can be viewed at wileyonlinelibrary.com]

Crystals of **1** are composed of two symmetry independent molecules. The OH group in the molecule around P2 is disordered on two sites, labeled O2A and O2B. In both compounds, the residues around the P-atoms are arranged in a trigonal-pyramidal fashion with average C−P−C angles slightly smaller than the ideal tetrahedral value, i.e., for **1**, P1: 102.5°, P2: 102.7° and for **3**, P1: 102.8°. Whereas in **3** classical hydrogen bonding is not observed, in **1** one O−H···O contact (O2B−H2B···O1) with a donor−acceptor distance of 3.16(2) Å and a bond angle of 162.9° is observed. This is in accordance with the behavior of the compound **1** in solution. A broad band at 3227 cm^{-1} and a sharp band at 3515 cm^{-1} was found in the IR spectrum of compound **1** [23], indicating an intramolecular hydrogen bond and the occurrence of free OH group, respectively [46]. Additionally, data obtained from the ^{1}H NMR spectrum of **1** at a concentration of 72.33 mM show a broad signal for the proton of the OH group at $\delta = 6.07$ ppm. Further measurements were done with half of the concentration showing a movement of the OH signal [47,48]. At a concentration of $c = 2.26$ mM, the OH group was found to be split to a doublet with coupling constant of $J = 6.0$ Hz at a chemical shift of $\delta = 6.01$ ppm. This is due to the coupling to the phosphorus. No cross peak of the OH-group to the respective proton in para position was found in the H,H-COSY. The results are outlined in Fig. 3 and in the Supporting Information.

To apply the ligation, phosphane **3** was reacted with three different azides **4–6** to obtain the desired Staudinger products **7–9**. Benzyl azide (**4**) gave the desired Staudinger product **7** [49], and the azide-functionalized glucose **5** as well as the amino acid **6** were reacted with **3** to yield **8** and **9**, respectively. The yields ranged from 78% to 86%. In general, phosphane oxide **10** was always obtained as a by-product in all reactions. To check other possible oxidation products, which could be formed during the Staudinger ligation, fluorinated phosphane oxide **11** was prepared from phosphane **3** which was treated with NaN_3. An overview of all reactions is given in Scheme 2.

Determination of k_{obs} via ^{19}F NMR

Studies on the reaction rate were performed to ensure that the reaction time of the traceless Staudinger ligation is suitable to apply for future ^{18}F radiolabeling. For analysis of the reaction times, it is necessary to distinguish between starting phosphane **3** and the Staudinger products **7–9**, based on their different ^{19}F chemical shifts pointed out in Fig. 4. The fluorine signal of starting material **3** was determined at $\delta = -106.1$ ppm and the signal of the Staudinger product **7** at $\delta = -110.4$ ppm in the ^{19}F NMR using a mixture of acetonitrile-d_6 and D_2O (ratio: v:v = 10:1). For comparison, the reactions were additionally monitored by "indirect" ^{31}P NMR measurements. The product **7** does not contain phosphorus, so the by-product **10** ($\delta = +35$ ppm) was detected instead in addition to the starting phosphane **3** ($\delta = -15$ ppm).

Our initial study comprised of three experiments. The first two were based on the equimolar reaction of both starting materials **3** and **4** at temperatures of 25 and 45°C, respectively. The low temperatures were chosen in consideration of future labeling reactions. Mild conditions are essential especially for labeling proteins or antibodies, which will denature or will be destroyed at elevated temperatures. For the third experiment, the reaction was performed with 10-fold excess of the starting azide **4** at 25°C to simulate conditions observed in radiolabeling procedures. Generally, the precursor (nonradioactive starting material) is always in high excess (100:1 to 1000:1) compared to the compound containing the radionuclide (radiolabeling building block) [31]. This leads to pseudo–first-order conditions for every radiolabeling reaction with noncarrier-added radionuclides (e.g., ^{18}F, ^{11}C, ^{99m}Tc). Owing to the azide **4** (as a prospective precursor) being 10-fold higher in concentration compared to the phosphane **3**, the pseudo–first-order conditions can also be supposed [50] and gives a good impression for the transfer to noncarrier-added radiolabeling conditions.

All NMR experiments were carried out in a mixture of acetonitrile-d_3 and D_2O (ratio: v:v = 10:1). A stock solution of phosphane **3** was prepared with a concentration of 71 nM. Solutions with azide **4** were prepared with final concentrations of 71 and 710 nM, respectively. At the beginning of the reaction, ^{19}F and

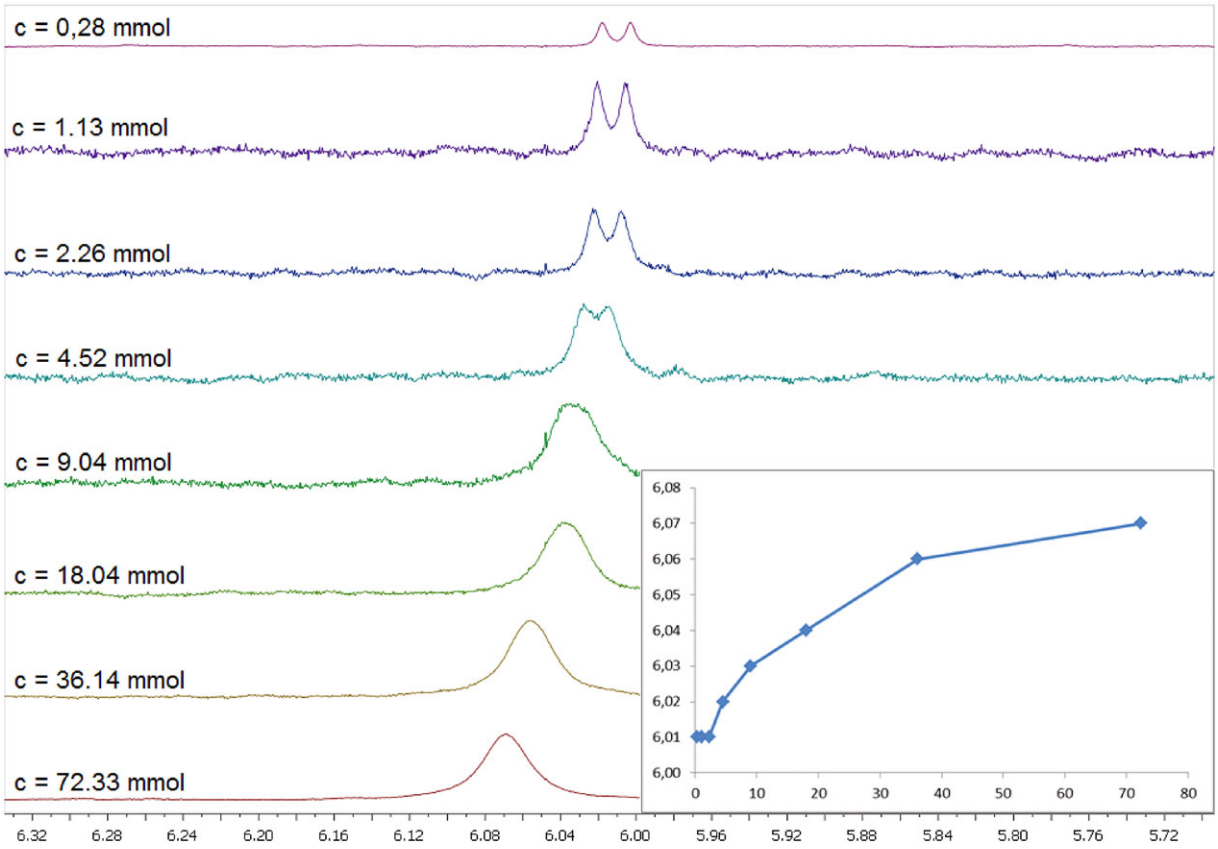

Figure 3 ^{1}H NMR spectra using different concentrations (spectra recorded in C_6D_6) and movement of the chemical shift of the OH group of compound **1** as a function of different concentrations (small figure). [Color figure can be viewed at wileyonlinelibrary.com]

^{31}P NMR spectra were recorded all 3–10 min, later all 30 min. A representative record of ^{19}F and ^{31}P NMR spectra for the reaction of **3** with **4** in 10-fold excess of **4** is displayed in Figs. 5 and 6.

To give a first impression on the Staudinger ligations reaction rate, the reaction half-live $\tau_{1/2}$ was determined. A summary of these data is found in Table I. When comparing the dependence on the temperature, the reaction rate at 45°C is higher. Thus, $\tau_{1/2} = 41.1$ min was found for the reaction at 45°C in contrast to $\tau_{1/2} = 203.8$ min for the reaction at 25°C. The same result is found when comparing the reaction (1:1 ratio) with the reaction (10:1 ratio) at 25°C. For the reaction with 10-fold excess of azide **4**, the shortest reaction half-life of $\tau_{1/2} = 22.2$ min was calculated. No starting material **3** was found after 92 min when using 10-fold excess of azide **4,** whereas starting material **3** from the equimolar reaction was still detectable after 350 min. The results are visualized in Fig. 7. Only slight differences between the results of the ^{19}F and the ^{31}P NMR measurements were observed.

Under the assumption that the reaction of phosphane **3** with a 10-fold excess of azide **4** behaves like a pseudo–first-order reaction, the rate constant k_{obs} was calculated according to the below equation [51]. With a concentration of 710 nM of azide **4**, k_{obs} is calculated with a value of 0.7×10^{-3} M^{-1} s^{-1}.

$$\tau_{1/2} = \frac{\ln 2}{k'} \quad \text{with: } k' = k_{obs} \cdot [\text{azide}]$$

Additionally, carbohydrate **5** was chosen, which contains a more sterically demanding N_3 group and reacted with phosphane **3** to give the Staudinger product **8**. The following NMR investigations were accomplished at 25 and 40°C with the 10-fold excess of azide **5**, indicating a slower reaction rate compared to the first reaction of **3** with **4**. A higher value for $\tau_{1/2}$ was found (53.7 min at 25°C and 20.2 min at 40°C), and the rate constant was calculated with $k_{obs} = 1.1 \times 10^{-3}$ M^{-1} s^{-1} (25°C) and $k_{obs} = 3.1 \times 10^{-3}$ M^{-1} s^{-1} (40°C).

Based on these results, the fructose derivative **6** with a spacer group between the fructose core and the azide

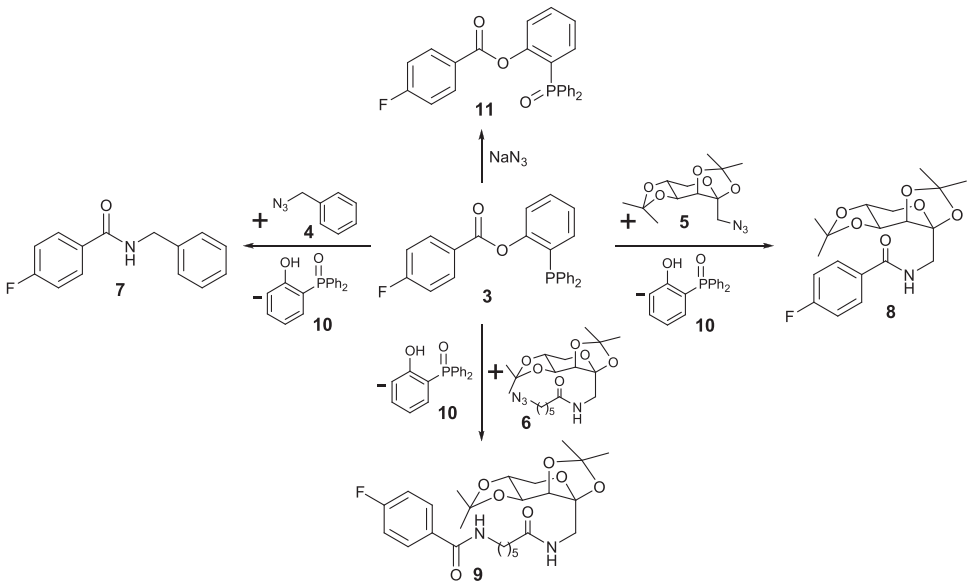

Scheme 2 Traceless Staudinger ligation of **3** with azides **4–6** to amide **7** and fructose derivatives **8** and **9**.

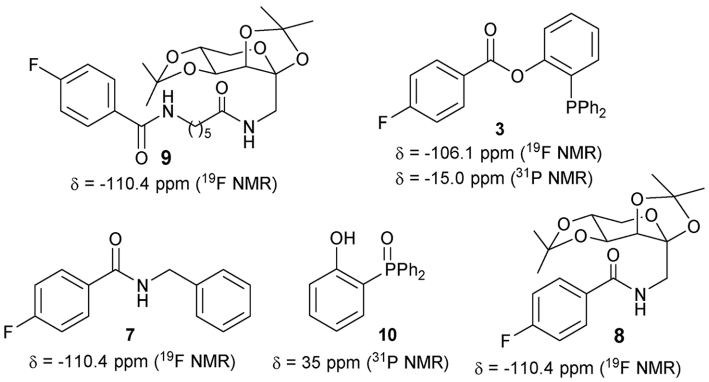

Figure 4 Chemical shifts of starting compound **3** and the products **7–10** in the ^{19}F and ^{31}P NMR (all samples measured in acetonitrile-d_3:D_2O = 10:1).

function was additionally prepared and reacted with phosphane **3** to give **9** under the aforementioned conditions. The reaction half-life $\tau_{1/2}$ was determined with 139 min at 25°C and 43 min at 40°C, and the reaction rate was calculated to be $k_{obs} = 0.5 \times 10^{-3}$ M^{-1} s^{-1} (25°C) and $k_{obs} = 1.5 \times 10^{-3}$ M^{-1} s^{-1} (40°C). Results are summarized in Table I.

All determined values for k_{obs} are in the similar range and in good agreement with other results found for the Staudinger ligation [34]. Although other bioorthogonal (click) reactions proceed faster [32], the traceless Staudinger ligation is readily suitable for radiolabeling purposes with fluorine-18 under mild reaction conditions.

CONCLUSION

X-ray structure determinations of the starting phosphanes and kinetic measurements of the reaction rate between fluorinated phosphane and various azides were accomplished under different reaction conditions to transfer and apply the traceless Staudinger ligation for future radiolabeling with short-lived β^+-emitter fluorine-18 and other radionuclides. For this purpose, ^{19}F NMR was used due to the presence of ^{19}F in the starting material (phosphane **3**) as well as in the corresponding products (**7–9**). The results of the measurements clearly indicate that it is possible to apply the traceless Staudinger ligation for radiolabeling purposes

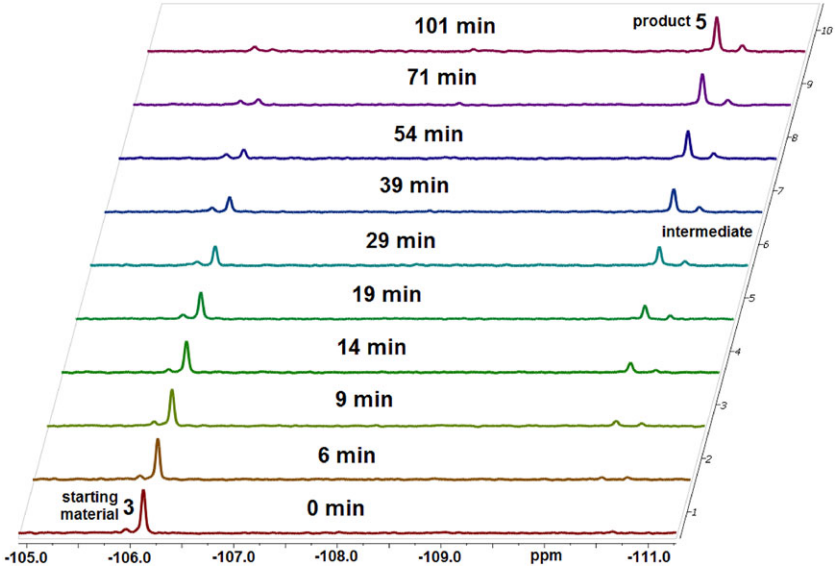

Figure 5 Representative set of ^{19}F NMR spectra recorded on different time points to determine the reaction half-life $\tau_{1/2}$ and the rate constant for the reaction of **3** with 10-fold excess of azide **4** at 25°C. [Color figure can be viewed at wileyonlinelibrary.com]

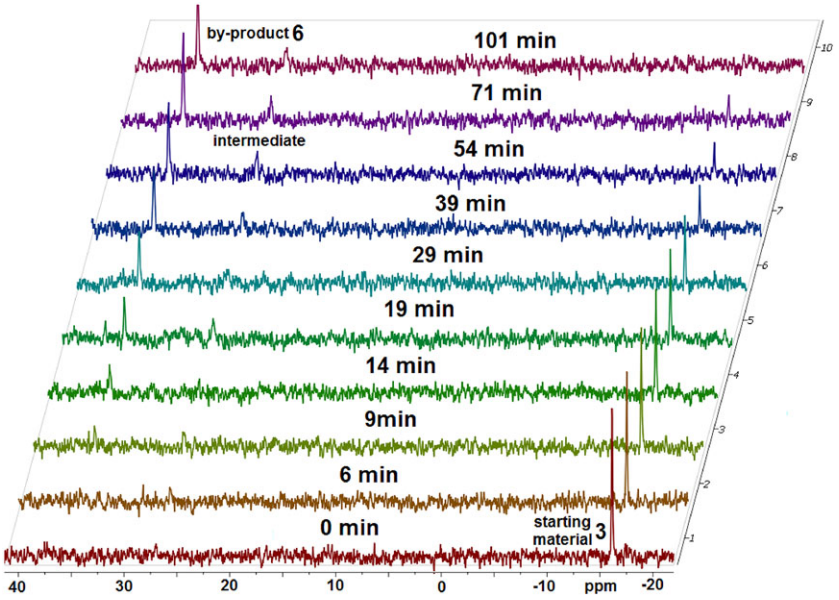

Figure 6 Representative set of ^{31}P-NMR spectra recorded on different time points for the reaction of **3** with 10-fold excess of azide **4** at 25°C. [Color figure can be viewed at wileyonlinelibrary.com]

Table 1 Summary of Results from NMR Measurements

Molar ratio of Starting Materials	Temperature	Reaction Half-Life $\tau_{1/2}$	k_{obs}
Phosphane 3: azide 4 = 1:1	25°C	203.8 ± 3.4 min	n.d.
Phosphane 3: azide 4 = 1:1	45°C	41.1 ± 1.2 min	n.d.
Phosphane 3: azide 4 = 1:10	25°C	22.2 ± 0.1 min	$0.7 \times 10^{-3} \pm 0.04 \times 10^{-3}$ $M^{-1}s^{-1}$
Phosphane 3: azide 5 = 1:10	25°C	53.7 ± 0.9 min	$1.1 \times 10^{-3} \pm 0.02 \times 10^{-3}$ $M^{-1}s^{-1}$
Phosphane 3: azide 5 = 1:10	40°C	20.2 ± 0.9 min	$3.1 \times 10^{-3} \pm 0.13 \times 10^{-3}$ $M^{-1}s^{-1}$
Phosphane 3: azide 6 = 1:10	25°C	129.4 ± 1.1 min	$0.5 \times 10^{-3} \pm 0.004 \times 10^{-3}$ $M^{-1}s^{-1}$
Phosphane 3: azide 6 = 1:10	40°C	43.8 ± 0.38 min	$1.5 \times 10^{-3} \pm 0.01 \times 10^{-3}$ $M^{-1}s^{-1}$

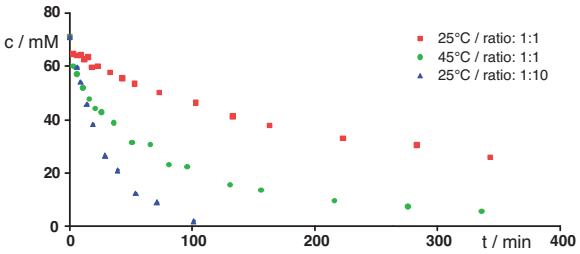

Figure 7 Decrease of concentration of phosphane **3** during Staudinger ligations at different temperatures and different ratios of starting materials **3** and **4**. [Color figure can be viewed at wileyonlinelibrary.com]

even in consideration of the short half-live of fluorine-18 under mild labeling conditions with a rather slow reaction rate.

Elisabeth Oberem (Universität Rostock) is gratefully acknowledged for her helpful discussions during the preparation of the manuscript.

BIBLIOGRAPHY

1. Wang, Z.-P. A.; Tiana, C.-L.; Zheng, J.-S. RSC Adv 2015, 7, 107192–107199.
2. Hermanson, G. T. Bioconjugate Techniques, 2nd ed.; Academic Press: London, 2008.
3. Patterson, D. M.; Nazarova, L. A.; Prescher, J. A. ACS Chem Biol 2014, 9, 592–605.
4. Bondalapati, S.; Jbara, M.; Brik, A. Nature Chem 2016, 8, 407–418.
5. Hadjiliadis, N. D. Cytotoxic, Mutagenic and Carcinogenic Potential of Heavy Metals Related to Human Environment; Springer Science+Business Media: Dordrecht, The Netherlands, 1997; 217 ff.
6. Köhn, M.; Breinbauer, R. Angew Chem, Int Ed 2004, 43, 3106–3116.
7. van Berkel, S. S.; van Eldijk, M. B.; van Hest, J. C. M. Angew Chem, Int Ed 2011, 50, 8806–8827.
8. Schilling, C. I.; Jung, N.; Biskup, M.; Schepers, U.; Bräse, S. Chem Soc Rev 2011, 40, 4840–4871.
9. Nilsson, B. L.; Kiessling, L. L.; Raines, R. T. Org Lett 2000, 2, 1939–1941.
10. Saxon, E.; Armstrong, J. I.; Bertozzi, C. R. Org Lett 2000, 2, 2141–2143.
11. Soellner, M. B.; Dickson, K. A.; Nilsson, B. L.; Raines, R. T. J AmChem Soc 2003, 125, 11790–11791.
12. Grandjean, C.; Boutonnier, A.; Guerreiro, C.; Fournier, J.-M.; Mulard, L. A. J Org Chem 2005, 70, 7123–7132.
13. Kleineweischede, R.; Hackenberger, C. P. R. Angew Chem, Int Ed 2008, 47, 5984–5988.
14. Liu, S.; Edgar, K. J. Biomacromolecules 2015, 16, 2556–2571.
15. Bianchi, A.; Bernardi, B. J Org Chem 2006, 71, 4565–4577.
16. Nisic, F.; Speciale, G.; Bernardi, A. Chem Eur J 2012, 18, 6895–6906.
17. David, O.; Meester, W. J. N.; Bieräugel, H.; Schoemaker, H. E.; Hiemstra, H.; van Maarseveen, J. H. Angew Chem, Int Ed 2003, 42, 4373–4375.
18. Masson, G.; den Hartog, T.; Schoemaker, H. E.; Hiemstra, H.; van Maarseveen, J. H. Synlett 2006, 865–868.
19. Pötzsch, R.; Fleischmann, S.; Tock, C.; Komber, H.; Voit, B. I. Macromolecules 2011, 44, 3260–3269.
20. Pretze, M.; Wuest, F.; Peppel, T.; Köckerling, M.; Mamat, C. Tetrahedron Lett 2010, 51, 6410–6414.
21. Pretze, M.; Flemming, A.; Köckerling, M.; Mamat, C. Z. Naturforsch B 2010, 65b, 1128–1138.
22. Mamat, C.; Franke, M.; Peppel, T.; Köckerling, M.; Steinbach, J. Tetrahedron 2011, 67, 4521–4529.
23. Mamat, C.; Köckerling, M. Synthesis 2015, 47, 387–394.
24. Tsao, M.-L.; Tian, F.; Schultz, P. G. ChemBioChem 2005, 6, 2147–2149.
25. Heldt, J.-M.; Kerzendörfer, O.; Mamat, C.; Starke, F.; Pietzsch, H.-J.; Steinbach, J. Synlett 2013, 432–436.
26. Wodtke, R.; König, J.; Pigorsch, A.; Köckerling, M.; Mamat, C. Dyes Pigm 2015, 113, 263–273.
27. Bräse, S.; Gil, C.; Knepper, K.; Zimmermann, V. Angew Chem, Int Ed 2005, 44, 5188–5240.
28. Debets, M. F.; van derDoelen, C. W. J.; Rutjes, F. P. J. T.; van Delft, F. L. ChemBioChem 2010, 11, 1168–1184.
29. Mamat, C.; Flemming, A.; Köckerling, M.; Steinbach, J.; Wuest, F. R. Synthesis 2009, 3311–3321.
30. Tam, A.; Soellner, M. B.; Raines, R. T. J Am Chem Soc 2007, 129, 11421–11430.
31. Saha, G. B. Fundamentals of Nuclear Pharmacy, 6th ed.; Springer: New York, 2010.
32. Pretze, M.; Pietzsch, D.; Mamat, C. Molecules 2013, 18, 8618–8665.
33. Richter, S.; Wuest, F. Molecules 2014, 19, 20536–20556.
34. Soellner, M. B.; Nilsson, B. L.; Raines, R. T. J Am Chem Soc 2006, 128, 8820–8828.
35. Lin, F. L.; Hoyt, H. M.; van Halbeek, H.; Bergman, R. G.; Bertozzi, C. R. J Am Chem Soc 2005, 127, 2686–2695.
36. Miller, P. W.; Long, N. J.; Vilar, R.; Gee, A. D. Angew Chem 2008, 120, 9136–9172.
37. Dolbier, W. R. Guide to Fluorine NMR for Organic Chemists, 1st Vol.; Wiley : Hoboken, NJ, 2009.
38. Rabenstein, D. L. Anal Chem 2001, 73, 214A–223A.
39. Martino, R.; Gilard, V.; Desmoulin, F.; Malet-Martino, M. J Pharm Biomed Anal 2005, 38, 871–891.
40. Campbell-Verduyn, L.; Elsinga, P. H.; Mirfeizi, L.; Dierckx, R. A.; Feringa, B. L. Org Biomol Chem 2008, 6, 3461–3463.
41. Sheldrick, G. M., SHELXS-97 and SHELXL-97, Programs for the Solution and Refinement of Crystal Structure; University of Göttingen: Göttingen, Germany, 1997.

42. Sheldrick, G. M. Acta Crystallogr C 2015, 71, 3–8.
43. Sheldrick, G. M. Acta Crystallogr A 2008, 64, 112–122.
44. Herd, O.; Heßler, A.; Hingst, M.; Tepper, M.; Stelzer, O. J Organomet Chem 1996, 522, 69–76.
45. Herd, O.; Heßler, A.; Hingst, M.; Machnitzki, P.; Tepper, M.; Stelzer, O. Catal Today 1998, 42, 413–420. Sheldrick, G. M. Acta Crystallogr C 2015, 71, 3–8.
46. Pavia, D. L.; Lapman, G. M.; Kritz, G. S. Introduction to Spectroscopy; Harcourt College: Orlando, FL, 2001, p. 45 ff.
47. Abraham, R. J; Mobli, M. Magn Reson Chem 2007, 45, 865–877.
48. Wendt, M. A.; Meiler, J.; Weinhold, F.; Farrar, T. C. Mol Phys 1998, 93, 145–152.
49. Mamat, C.; Flemming, A.; Köckerling, M. Z. Kristallogr. NCS 2010, 225, 345–346.
50. Anslyn, E. V.; Dougherty, D. A. Modern Physical Organic Chemistry; University Science Books: USA, 2005.
51. Levine, I. N. Physical Chemistry, 4th ed.; McGraw-Hill: New York, 1995, chapt. 17.